



INFLUENCES OF DEPOSITION LAYER ON THE PROPERTIES OF TITANIUM DIOXIDE THIN FILMS FABRICATED BY DIP COATING TECHNIQUE

Anis Suhaili Bakri, Mohd Zainizan Sahdan, Feri Adriyanto, Nor Damsyik Mohd Said and Amaliyana Raship

Microelectronics and Nanotechnology- Shamsuddin Research Centre, Malaysia

Faculty of Electrical and Electronic Engineering, Universiti Tun Hussein Onn Malaysia, Parit Raja, Batu Pahat, Johor, Malaysia

E-Mail: zainizno@gmail.com

ABSTRACT

Titanium dioxide (TiO_2) thin films were deposited on silicon substrates by using a sol-gel dip coating technique. In order to study the influences of the deposition layer on the properties of TiO_2 films, the number of layer was varied. Then, the TiO_2 films were analyzed by X-ray diffraction (XRD), field emission scanning electron microscope (FESEM) and four-point probe. Generally, all films are uniform without the presence of any grain or grain boundary. The TiO_2 films were confirmed by energy-dispersive X-ray spectroscopy (EDS) which indicates the presence of titanium (Ti) and Oxygen (O). It was found that, the thickness and crystallite size of the films increases as the deposition layers increased. On the contrary, the resistivity of the TiO_2 films decreases in the range of $5.80 \times 10^2 \Omega \cdot \text{cm}$ and $1.45 \times 10^2 \Omega \cdot \text{cm}$ as the deposition layer increased. Therefore, it has been determined that the properties of TiO_2 films were strongly correlated with the thickness of the films.

Keywords: TiO_2 film, sol-gel dip coating, crystal structure.

INTRODUCTION

Titanium also known as titania has a wide band gap energy and is a non-toxic material. The band gap energy is different according to their crystallographic polymorphs of the titanium dioxide (TiO_2). TiO_2 are extensively studied because of their interesting properties such as high photocatalytic activity, high refractive index, and good physical and chemical stability (Ahn, Kim, Kim, & Hahn, 2003). The unique properties of the TiO_2 make this metal oxides material suitable for many applications, particularly as dye-sensitized solar cells (Moon, Sung, and Han, 2013), gas sensor (Castañeda, López-Suárez, and Tiburcio-Silver, 2010), white pigment for paints (Valencia *et al.*, 2010) and photocatalyst (Hanaor and Sorrell, 2011). TiO_2 has three different crystallographic polymorphs which is rutile (tetragonal), anatase (tetragonal), and brookite (orthorhombic) (Diebold, 2003; Fröschl *et al.*, 2012; Luís, Neves, Mendonça, and Monteiro, 2011). Rutile have been reported as the stable phase while anatase and brookite are metastable phase (Di Paola, Bellardita, and Palmisano, 2013). In high temperature ($\sim 1300^\circ\text{C}$ and above) (Hanaor and Sorrell, 2011), the anatase and brookite which is metastable form are readily transformed to rutile. The band gap energy of rutile is 3.02 eV, anatase is 3.23 eV and brookite is 3.14 eV (Di Paola *et al.*, 2013).

TiO_2 thin films have been fabricated on several kind of substrates such as Indium Tin Oxide (ITO), glass (Paez and Matoušek, 2004), alumina, silicon and even on substrate with low thermal resistance like plastics and textiles (Sisti *et al.*, 2012). In this work, silicon have been used due to its special features such as available in large diameter and have good electrical and thermal properties (Pal and Jacob, 2004).

Different techniques have been used for the fabrication of TiO_2 such as reactive magnetron sputtering

(Piwo, Kisielowska, Szczukocki, Krawczyk, and Sielski, 2014), chemical vapor deposition (Zheng, Gu, Sun, Mo, and Chen, 2010), spray pyrolysis (Castañeda *et al.*, 2010), hydrothermal (Wang, Li, Zhi, Manivannan, and Wu, 2008) and sol-gel method. Among of these technique, the sol-gel method has some advantages such as reproducibility (Mechiakh, Sedrine, Chtourou, and Bensaha, 2010), can deposited large area of substrate, can control film thickness and easy control of chemical composition of thin film layers (Sonawane, Kale, and Dongare, 2004). Sol-gel coating method has been classified as two different methods such as spin coating and dip coating. The dip coating have been widely used for fabricated TiO_2 nanostructured thin films (Barati, Sani, Ghasemi, Sadeghian, and Mirhoseini, 2009; K, Ramli, Amri, and Maarof, 2012; Mechiakh *et al.*, 2010).

In this paper, we report the influence of deposition layers of TiO_2 films on the surface morphology, structural and electrical properties.

EXPERIMENTAL PROCEDURE

Preparation of the coating solution

Flow chart of the experiment is shown in Figure-1. A starting solution for the dip coating process was prepared from titanium (IV) butoxide $\text{Ti}(\text{OC}_4\text{H}_9)_4$ (97%, Sigma Aldrich) as a precursor and ethanol as a solvent. Precursor solutions for TiO_2 films were prepared by the following method: at room temperature titanium (IV) butoxide and glacial acetic acid were dissolved in ethanol. Deionized water was added to the solution under continuous stirring. The mixture was stirred and heated to 40°C for about 10 minutes. The reaction process between the materials in the solution were increased during the heating process. Then the solution was continuously



stirred at a constant speed for 3 hours to complete the reaction.

Deposition of thin films

For the deposition of the film, a single sided polished n-type silicon wafer (500 μm thick, (100) orientation, obtained from semiconductor wafer, inc.) were used as a substrate. The substrate were cut in to (20 mm X 30 mm). Silicon substrates were cleaned with diluted hydrofluoric acid (HF) (HF-water) with molar ratio of 1:10 before depositing the films to remove native oxide from the substrates. The substrates were then washed with deionized water and dried with nitrogen (N_2) gas. Afterwards, the substrates were dipped and withdrawn from the precursor solution at a withdrawal speed of 180 mm/min by using a dip coater machine (PTL-MM01 Desktop Dip Coater). Immediately after dipping process, the sample was pre-heated at 100 $^{\circ}\text{C}$ for 5 minutes in hot plate. The process was repeated for several times to obtain a desired coating. Finally, the sample was annealed at 500 $^{\circ}\text{C}$ for 1 hour in furnace to improve the structural property.

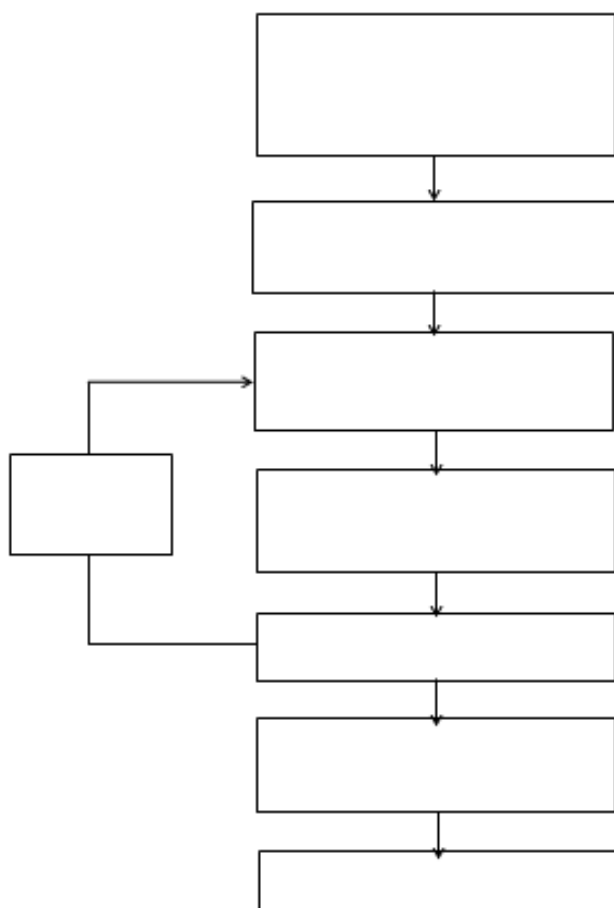


Figure-1. The flowchart of the experiment methodology.

Surface characterization

The TiO_2 films on silicon substrates were characterized for crystalline properties using X-ray diffractometer (XRD, model; PANalytical X-Pert Powder)

with a Cu- $\text{K}\alpha$ radiation source at a setting of 40mA and 40 kV. The diffraction patterns were collected in the range $2\theta = 20^{\circ}$ - 70° with a 0.01° step size. The surface morphology of the coating layer was characterized using Field Emission Scanning Electron Microscope (FESEM, model; JSM-7600F) with an accelerating voltage of 15kV. Approximate film thickness was measured by using Alpha-Step IQ Surface Profiler (KLA Tenkor) with scan length 4000 μm and scan speed 50 $\mu\text{m/s}$ while the resistivity of the thin films were measured by using four point probe.

RESULTS AND DISCUSSIONS

Structural properties

To compare the effect of different deposition layer on structural properties of TiO_2 films, the films were fabricated on the silicon substrates by the dip-coating method. Figure-2 shows the XRD pattern in the range of $2\theta = 20^{\circ}$ - 70° of the samples with 5, 7, 9 and 11 layers. Measurements with XRD confirmed that anatase with tetragonal lattice structure is the only crystalline phase present for each layer. All peaks match well with Bragg reflections of the standard anatase nanocrystalline structure (ICSD file no. 98-015-4604). A weak silicon peak was also observed in all samples at position $2\theta = 52.4^{\circ}$ (ICSD file no. 98-004-1991).

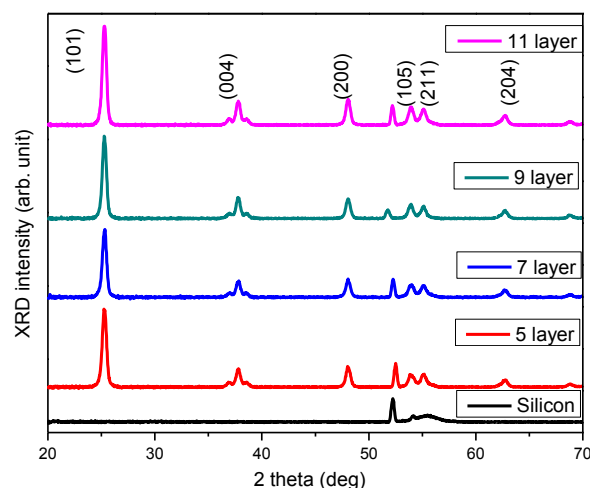


Figure-2. XRD pattern of TiO_2 films with different deposition layer.

Strong XRD peaks corresponding to TiO_2 anatase (101) were clearly observed at $2\theta = 25.2^{\circ}$, along with generally low intensities of 2θ values at about 37.6° (004), 48.0° (200), 53.9° (105), 55.2° (211), and 62.7° (204) diffraction peaks. The increase in the intensity of these peaks indicates an improvement of the crystalline structure, by a rearrangement phenomenon and the increase in TiO_2 particle size (Luís *et al.*, 2011). From the results, it can be seen that the intensities of the anatase TiO_2 (101) peak were increased as the 9 deposition layers of the film is increased to 11 deposition layers. This can be



explained by the improvement of the crystal quality. In fact, the improvement of the crystal quality may be due to

the increase of the film thickness.

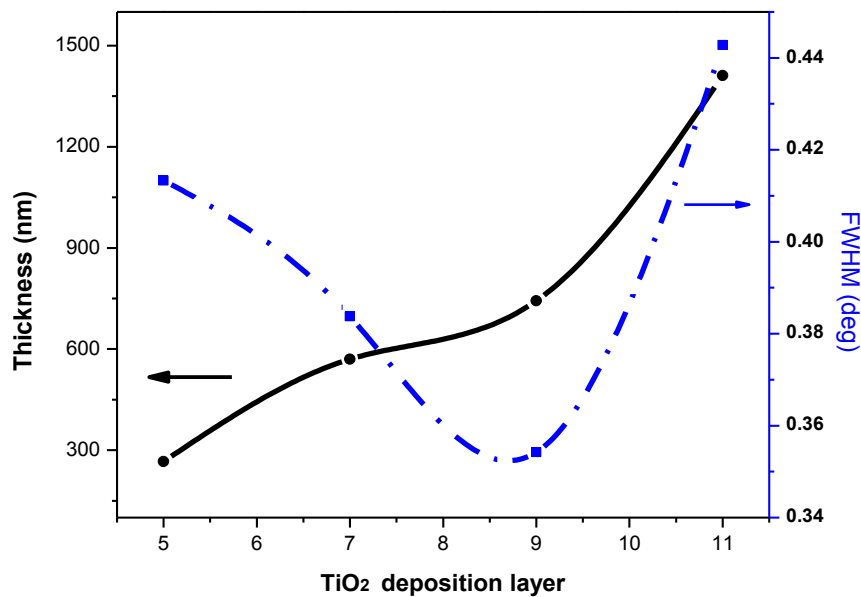


Figure-3. Variation of thickness and FWHM at various TiO₂ films.

Table-1. Evaluated structural parameters of TiO₂ films.

TiO ₂ layer	Position (2 θ°)	FWHM, deg	Crystallite size, d (nm)	Thickness (nm)
5	25.2	0.4133	22.47	265.86
7	25.3	0.3838	24.25	569.93
9	25.2	0.3542	26.33	743.39
11	25.3	0.4428	20.94	1411.29

The thickness of each sample was characterized using surface profiler. It can be seen that the average thickness of the thin film were changed from 265.86 nm to 569.93 nm, 743.39 nm, and 1411.29 nm for 5, 7, 9 and 11 deposition layers, respectively. These results agree well with those of the increasing peak intensity as a function of deposition layer at the XRD measurements.

Figure-3 shows the thickness and full width at half maximum (FWHM) values of the anatase TiO₂ (101) peak as a function of TiO₂ deposition layers. From the figure, it can be seen that when the deposition layer is increased the thickness also increases while from the XRD

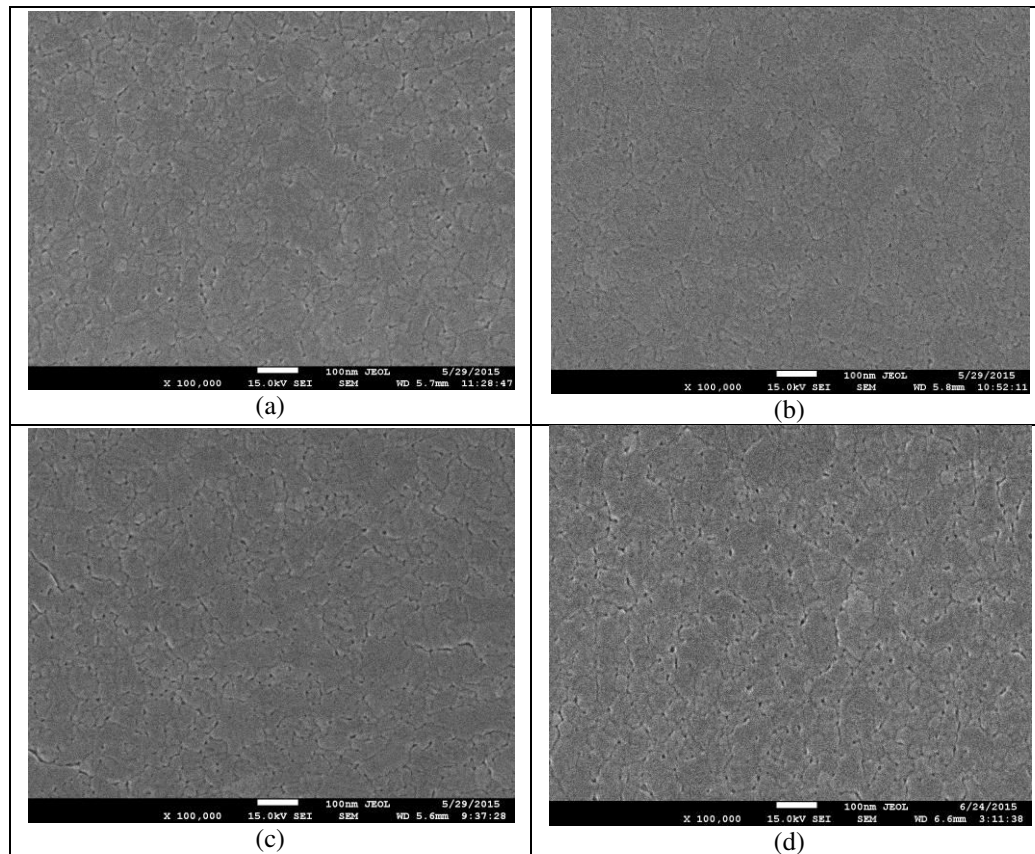
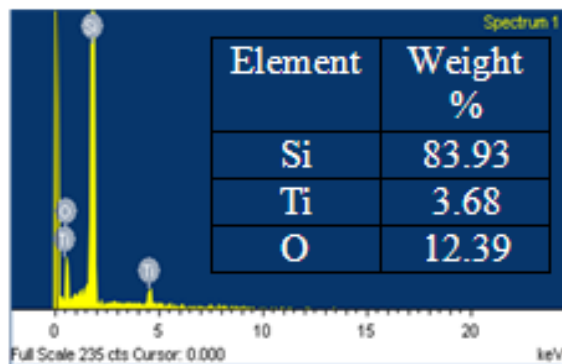
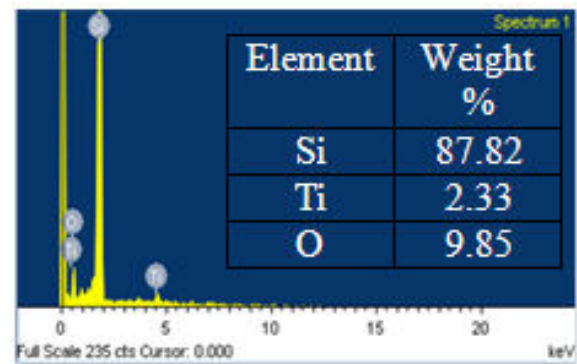


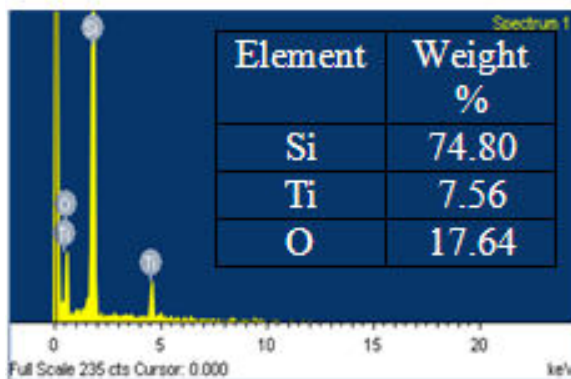
Figure-4. FESEM images for different layer dip coating (a) 5 layer (b) 7 layer (c) 9 layer (d) 11 layer.



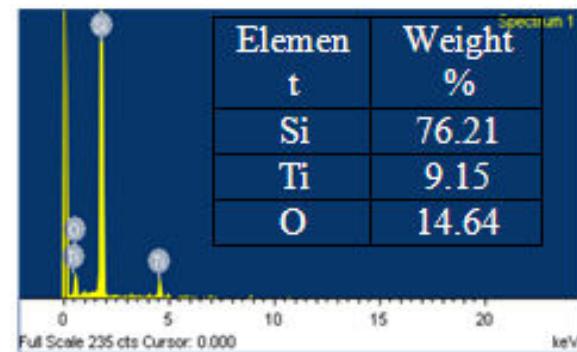
(a)



(b)



(c)



(d)

Figure-5. EDS images for different layer dip coating (a) 5 layer (b) 7 layer (c) 9 layer (d) 11 layer.



data, it is also observed that the FWHM decreases with an increase in deposition layers and approaches a minimum value at 9 layers deposition (film thickness at - 743 nm). As the film thickness increase further, the width of the peaks increase. This information indicates an increase in the crystallite size of the TiO₂ thin films was produced at higher deposition layer.

The crystal quality was improved by increasing the deposition layers. The average crystallite size of anatase TiO₂ (101) at $2\theta = 25.2^\circ$ was estimated from the FWHM of the XRD peak using Scherrer's formula (Malek *et al.*, 2013).

$$d = \frac{k\lambda}{\beta \cos \theta} \quad (1)$$

Where d is the crystallite diameter of TiO₂ thin film, k is the shape constant (0.94), λ is the wavelength of X-Ray (CuK α = 1.5406 Å), θ is the Bragg angle and β is the observed peak width at half-maximum peak height. The TiO₂ crystallite size values estimated during this work are presented in Table-1. The calculated values of the crystallite sizes changed from 22.47 nm to 26.33 nm. It is observed that the crystallite size increases with an increase in the deposition layer. However, for 11 layer of TiO₂ films, the crystallite size decreased.

Morphological properties

Figure-4 shows the FESEM images at 100 k magnification with 15 kV applied voltage of the TiO₂ films prepared on silicon substrates, corresponding to the deposited layer of 5, 7, 9 and 11 layers. It can be seen that TiO₂ films with different deposition layer (Figure-4 (a-d)) show almost similar morphology. There is no obvious grain or grain boundary on the sample. (Figure-5 (a-d)) show the energy-dispersive X-ray spectroscopy (EDS) spectrum indicating the presence of Titanium (Ti), Oxygen (O) and Silicon (Si) element. A high peaks of Si in all samples resulting from the silicon substrate. Thus, prove that TiO₂ has been formed as being supported by XRD data in Figure-2.

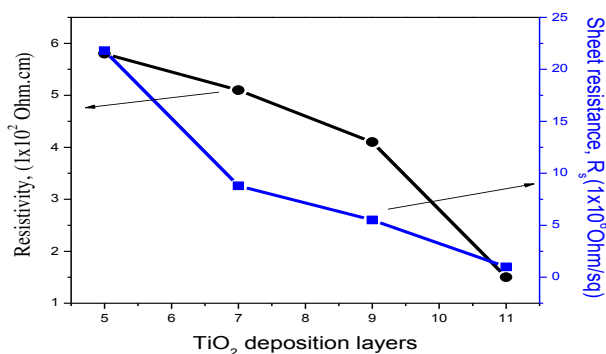


Figure-6. Variation of resistivity and sheet resistance at various TiO₂ thin films.

Figure-6 shows the resistivity and sheet resistance of TiO₂ thin film as a function of TiO₂

deposition layers. The resistivity and the sheet resistance of the TiO₂ films appear to be decreasing with the increment of the deposited layer of the TiO₂ films. The 11 layers deposition which is the highest deposition layers shows the lowest resistivity (1.45×10^{-2} Ω.cm) and sheet resistance (2.6×10^6 Ω/sq) compared to others. The resistivity is calculated using the formula below:

$$\rho = 2\pi s \frac{V}{I} \quad (2)$$

Where ρ is the resistivity, s is the spacing between the probe, V is the voltage and I is the current. The sheet resistance is measured by four-point probe. The sheet resistance can be determined based on the resistivity and thickness of the films according to the equation:

$$R_s = \frac{\rho}{t} \quad (3)$$

Where ρ is the resistivity and t is the thickness. The conductivity of the TiO₂ thin film is the reciprocal of the resistivity as shown by the following equation:

$$\sigma = \frac{1}{\rho} \quad (4)$$

Where σ is the conductivity and ρ is the resistivity. The samples were deposited from 5 until 11 layers indicate improvements of the conductivity according to the deposition layer applied. The highest conductivity can be found at thin film with 11 deposition layers. This is may be due to the improvement of the anatase TiO₂ crystal quality. When the crystal quality is improve, the electron movement from one particles to another improve.

The growth rate of the TiO₂ films deposited with 5 layers deposition is small compared to the growth rate deposited with 11 layers deposition. When this phenomenon occurs which is at 11 layers deposition, the empty space around the particles is reduced, causing a more physical contact within the film that resulted in decrease the resistivity of the films, as has been shown previously.

CONCLUSIONS

TiO₂ thin films have been successfully prepared by sol-gel dip coating method and the effect of deposition layer on their structural and electrical properties were examined. It was found that the TiO₂ films were primarily composed of anatase-phase TiO₂. The crystalline quality of the films improves at 11 layer deposition. Based on Scherrer's formula calculations, the crystallite size of the anatase phase increased from 22.47 nm to 26.33 nm with increasing deposition layer from 5 to 9 layers. With increasing the deposition layer from 5 to 11 layers, the resistivity of TiO₂ films decreased from 5.80×10^{-2} Ω.cm to 1.45×10^{-2} Ω.cm due to the improvement in the crystallinity. The results show that the deposition layer



clearly affects the structural and electrical properties of TiO₂ films.

ACKNOWLEDGEMENT

The author would like to thank Malaysia Ministry of Higher Education for providing research funding support under Prototype Research Grant Scheme (PRGS) Vote Number G005.

REFERENCES

- Ahn, Y. U., Kim, E. J., Kim, H. T. and Hahn, S. H. 2003. Variation of structural and optical properties of sol-gel TiO₂ thin films with catalyst concentration and calcination temperature. *Materials Letters*, 57, 4660-4666. doi:10.1016/S0167-577X(03)00380-X.
- Barati, N., Sani, M. a F., Ghasemi, H., Sadeghian, Z. and Mirhoseini, S. M. M. 2009. Preparation of uniform TiO₂ nanostructure film on 316L stainless steel by sol-gel dip coating. *Applied Surface Science*, 255, 8328-8333. doi:10.1016/j.apsusc.2009.05.048.
- Castañeda, L., López-Suárez, and Tiburcio-Silver, a. 2010. Influence of colloidal silver nanoparticles on the novel flower-like titanium dioxide oxygen sensor performances. *Journal of Nanoscience and Nanotechnology*, 10(2), 1343-1348. doi:10.1166/jnn.2010.1839.
- Di Paola, A., Bellardita, M. and Palmisano, L. 2013. Brookite, the Least Known TiO₂ Photocatalyst. *Catalysts*, 3(1), 36-73. doi:10.3390/catal3010036.
- Diebold, U. 2003. The surface science of titanium dioxide. *Surface Science Reports*, 48(5-8), 53-229. doi:10.1016/S0167-5729(02)00100-0.
- Fröschl, T., Hörmann, U., Kubiak, P., Kučerová, G., Pfanzelt, M., Weiss, C. K., Wohlfahrt-Mehrens, M. 2012. High surface area crystalline titanium dioxide: potential and limits in electrochemical energy storage and catalysis. *Chemical Society Reviews*, 41(15), 5313. doi:10.1039/c2cs35013k.
- Hanaor, D. a H., & Sorrell, C. C. 2011. Review of the anatase to rutile phase transformation. *Journal of Materials Science*, 46(4), 855-874. doi:10.1007/s10853-010-5113-0.
- K, N. F. A., Ramli, M. Z., Amri, N. and Maarof, H. I. 2012. Hydrophilic of SiO₂ / TiO₂ Double Layers Thin Film Prepared by Sol-gel Dip Coating Method. In *IEEE Symposium on Humanities, Science and Engineering Research* (pp. 53-57).
- Luís, A. M., Neves, M. C., Mendonça, M. H. and Monteiro, O. C. 2011. Influence of calcination parameters on the TiO₂ photocatalytic properties. *Materials Chemistry and Physics*, 125(1-2), 20-25. doi:10.1016/j.matchemphys.2010.08.019.
- Malek, M. F., Mamat, M. H., Sahdan, M. Z., Zahidi, M. M., Khusaimi, Z. and Mahmood, M. R. 2013. Influence of various sol concentrations on stress/strain and properties of ZnO thin films synthesised by sol-gel technique. *Thin Solid Films*, 527, 102-109. doi:10.1016/j.tsf.2012.11.095.
- Mechiakh, R., Sedrine, N. Ben, Chtourou, R. and Bensaha, R. 2010. Correlation between microstructure and optical properties of nano-crystalline TiO₂ thin films prepared by sol-gel dip coating. *Applied Surface Science*, 257(3), 670-676.
- Moon, B.-H., Sung, Y.-M. and Han, C.-H. 2013. Titanium oxide Films Prepared by Sputtering, Sol Gel and Dip Coating Methods for Photovoltaic Application. *Energy Procedia*, 34, 589-596. doi:10.1016/j.egypro.2013.06.789.
- Paez, L. R. and Matoušek, J. 2004. Properties of sol-gel tio₂ layers on glass substrate, 48(2), 66-71.
- Pal, S. and Jacob, C. 2004. Silicon - A new substrate for GaN growth. *Bulletin of Materials Science*, 27(6), 501-504. doi:10.1007/BF02707276.
- Piwo, I., Kisielewska, A., Szczukocki, D., Krawczyk, B. and Sielski, J. 2014. *Applied Surface Science* The photoactivity of titanium dioxide coatings with silver nanoparticles prepared by sol - gel and reactive magnetron sputtering methods – comparative studies, 288, 503-512.
- Sisti, L., Cruciani, L., Totaro, G., Vannini, M., Berti, C., Tobaldi, D. M., ... Commereuc, S. 2012. TiO₂ deposition on the surface of activated fluoropolymer substrate. *Thin Solid Films*, 520(7), 2824-2828. doi:10.1016/j.tsf.2011.10.046.
- Sonawane, R. S., Kale, B. B. and Dongare, M. K. 2004. Preparation and photo-catalytic activity of Fe-TiO₂ thin films prepared by sol-gel dip coating. *Materials Chemistry and Physics*, 85(3), 52-57. doi:10.1016/j.matchemphys.2003.12.007.
- Wang, J., Li, M., Zhi, M., Manivannan, A. and Wu, N. 2008. Hydrothermal Synthesis and Photocatalytic Activity of Titanium Dioxide Nanotubes, Nanowires and Nanospheres. In *MRS Proceedings* (Vol. 1144, pp. 1144-LL07-08). doi:10.1557/PROC-1144-LL07-08.
- Zheng, K., Gu, L., Sun, D., Mo, X. and Chen, G. 2010. The properties of ethanol gas sensor based on Ti doped ZnO nanotetrapods. *Materials Science and Engineering B: Solid-State Materials for Advanced Technology*, 166, 104-107. doi:10.1016/j.mseb.2009.09.029.